Integrative Genomic Analysis of Aneuploidy in Uveal Melanoma

Justis P. Ehlers,[1] Lori Worley,[2] Michael D. Onken,[2] and J. William Harbour[2]

Abstract

Purpose: Aneuploidy is a hallmark of cancer and is closely linked to metastasis and poor clinical outcome. Yet, the mechanisms leading to aneuploidy and its role in tumor progression remain poorly understood. The extensive and complex karyotypic abnormalities seen in many solid tumors could hinder the identification of pathogenetically relevant chromosomal alterations. Uveal melanoma is an attractive solid tumor for studying aneuploidy because it is a relatively homogeneous cancer that is highly metastatic and has low nonspecific chromosomal instability.

Experimental Design: Comparative genomic hybridization and gene expression profiling were used to analyze patterns of aneuploidy in 49 primary uveal melanomas. This analysis was supplemented by a review of cytogenetic findings in 336 published cases.

Results: Three prognostically significant tumor subgroups were identified based on the status of chromosomes 3 and 6p. Discrete patterns of chromosomal alterations accumulated in these three subgroups in a nonrandom temporal sequence. Poor clinical outcome was associated with early chromosomal alterations rather than overall aneuploidy. A gene expression signature associated with aneuploidy was enriched for genes involved in cell cycle regulation, centrosome function, and DNA damage repair. One of these genes was *PTEN*, a tumor suppressor and genomic integrity guardian, which was down-regulated in association with increasing aneuploidy ($P = 0.003$).

Conclusions: The relationship between aneuploidy and poor prognosis may be determined by specific, pathogenetically relevant chromosomal alterations, rather than overall aneuploidy. Such alterations can be identified using integrative genomic methods and may provide insights for novel therapeutic approaches.

Aneuploidy is a hallmark of cancer and a marker of poor clinical outcome (1). However, the mechanisms leading to aneuploidy and its role in tumor progression remain poorly understood, particularly in solid tumors. Some hematopoietic malignancies exhibit specific chromosomal rearrangements that are causally linked to tumor progression, but this is uncommon in solid tumors, which frequently exhibit widespread and complex karyotypic changes. Most of these changes are likely to be nonspecific by-products of chromosomal instability, hindering the identification of pathogenetically relevant alterations (2). The study of aneuploidy is further complicated by the recognition that cytogenetic changes in cultured tumor cells, which are required for traditional karyotype analysis, may not accurately reflect those of the whole primary tumor (3).

To circumvent some of these shortcomings, we have used integrative genomic techniques to study aneuploidy in primary tumor samples from a single cancer type. Uveal melanoma (UM) is an attractive solid tumor for studying aneuploidy because it is remarkably uniform in its clinical, histopathologic, and genetic features, and it metastasizes in up to 50% of patients (4, 5). UM displays recurrent chromosomal rearrangements but less generalized chromosomal instability than many other solid tumors (6, 7).

In this study, genome-wide comparative genomic hybridization and gene expression profiling were used to analyze 49 primary UMs in a cohort of patients after an extensive clinical follow-up. This analysis was supplemented by cytogenetic data collected from 336 UMs reported in the literature. Most aneuploidy occurred in the form of discrete patterns of chromosomal alterations that accumulated in a nonrandom temporal sequence. Three subtypes of UM based on aneuploidy pattern were identified and correlated with clinical outcome. Gene expression profiling detected a signature associated with aneuploidy and identified loss of *PTEN* expression as a marker of aneuploidy.

Materials and Methods

Tumor samples and cytogenetic data. This study was approved by the Institutional Review Board of Washington University. Cytogenetic

Authors' Affiliations: [1]Wills Eye Hospital, Philadelphia, Pennsylvania and [2]Department of Ophthalmology and Visual Sciences, Washington University, St. Louis, Missouri

Received 7/25/07; revised 9/25/07; accepted 10/12/07.

Grant support: National Cancer Institute (R01 CA125970), Tumori Foundation, Horncrest Foundation, Barnes-Jewish Hospital Foundation, and Research to Prevent Blindness, Inc.

The costs of publication of this article were defrayed in part by the payment of page charges. This article must therefore be hereby marked *advertisement* in accordance with 18 U.S.C. Section 1734 solely to indicate this fact.

Note: Supplementary data for this article are available at Clinical Cancer Research Online (http://clincancerres.aacrjournals.org/).

Requests for reprints: J. William Harbour, Box 8069, 660 South Euclid Avenue, Washington University School of Medicine, St. Louis, MO 63110. Phone: 314-362-3315; Fax: 314-747-5073; E-mail: harbour@wustl.edu.

doi:10.1158/1078-0432.CCR-07-1825

analysis of 49 primary UMs obtained at enucleation was done using data obtained from array-based comparative genomic hybridization using human bacterial artificial chromosome arrays, as previously described (8). Inclusion criteria included pathology-verified diagnosis of primary UM. Exclusion criteria included history of ocular brachytherapy or extensive tumor necrosis, both of which confound the interpretation of DNA and RNA profiling. Chromosomal arms were scored as loss (mean $\log_2$ ratio < -0.5), normal (-0.5 ≤ mean $\log_2$ ratio < 0.5), or gain (mean $\log_2$ ratio ≥ 0.5). These thresholds were previously established and validated (8, 9). This analysis was expanded by the inclusion of 336 tumors from 13 publications (10–22). Cases were included if cytogenetic data were generated using karyotypic analysis, comparative genomic hybridization, PCR, microsatellite analysis, fluorescence *in situ* hybridization, or loss of heterozygosity. Exclusion criteria included publications that did not provide cytogenetic data on individual tumors and lack of data on the status of chromosome 3. Each chromosome (or chromosomal arm when available) was scored as loss, normal, or gain. Sufficient information was available for analysis of the following chromosomes and chromosomal arms: 1, 3, 6p, 6q, 8p, 8q, 9p, 11, 13q, 14, 16q, 17p, 18q, 20q, 21, and 22. To maximize the data available for analysis, all cytogenetic information were included from each article, even though some articles did not evaluate all of the chromosomes. Aneuploidy was calculated as the fraction of nondiploid chromosomal arms. The cumulative fraction of nondiploid chromosomal arms was calculated as a function of overall aneuploidy using Microsoft Excel 2003. A self-organizing map algorithm available on GeneCluster version 2.0 was used as an unsupervised method for detecting clusters of covarying chromosomal alterations.

Gene expression profiling. Gene expression signatures were available for 43 of the tumors in this study and had been assigned as class 1 (favorable prognosis) or class 2 (poor prognosis), as previously described (8, 23). Gene expression values obtained on Illumina Ref8 BeadChips were available for 25 tumors and were subjected to rank-invariant normalization using BeadStation software and filtered for a median significance level of $P < 0.05$. Principal component analysis was done using Spotfire software.[3] Differentially expressed genes were identified using significance analysis of microarrays (SAM).[4] SAM variables were initially calibrated to generate a gene list with a 20% false discovery rate, which resulted in 13 up-regulated genes and 1,271 down-regulated genes. For down-regulated genes, a more stringent cutoff of <10% false discovery rate was selected, which reduced the list to 512 genes. These genes were further screened by signal-to-noise ratio using GeneCluster version 2.0,[5] which resulted in 30 genes with a threshold score of ≥1.4. The resulting gene set was analyzed with the Gene Set Analysis module of SAM to identify curated gene sets in the "c2" database[6] that were significantly associated with our gene set.

Statistical analysis. Associations between aneuploidy, specific chromosomal alterations, and clinicopathologic variables were tested for statistical significance using the Fisher exact test and Mann-Whitney test as appropriate. Survival analysis was done by Kaplan-Meier analysis. All calculations were done using MedCalc version 9.2.0.2.

Results

Clinical, pathologic, and genetic variables are summarized in Supplementary Table S1. Genome-wide array comparative genomic hybridization was done on 49 primary UMs, and chromosomal arms were analyzed for copy number variations (CNV; Fig. 1A). Discrete, recurrent CNVs were observed with low levels of random, background aneuploidy, measured as the fraction of nondiploid chromosome arms per tumor, ranged from 0.0 to 0.39 (mean, 0.15; median, 0.13). There was no association between aneuploidy and patient age ($P = 0.867$), gender ($P = 0.705$), ciliary body involvement ($P = 0.118$), cytologic severity ($P = 0.151$), tumor diameter ($P = 0.659$), or tumor thickness ($P = 0.116$). Aneuploidy was prognostically significant when comparing tumors with minimal aneuploidy (<5% chromosomal arms with CNVs) to those with greater aneuploidy (Kaplan-Meier, $P = 0.05$; Fig. 1B). Importantly, however, further subdivision of tumors based on greater amounts of aneuploidy did not show prognostic significance (Table 1), suggesting that the association between aneuploidy and poor clinical outcome was determined by early chromosomal alterations rather than overall aneuploidy.

A self-organizing map algorithm was used as an unsupervised technique to identify covarying chromosomal CNVs. Initially, the analysis was done with only two windows to identify major clusters based on CNV. One cluster consisted of seven

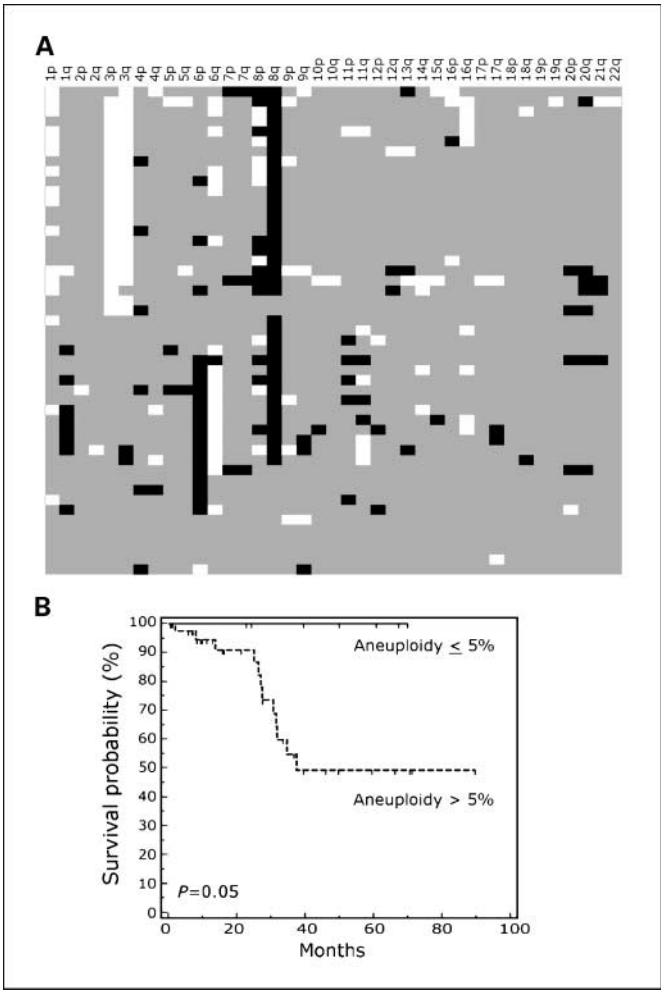

Fig. 1. CNV detected by array CGH in 49 primary uveal melanomas. *A,* heatmap showing CNVs by chromosomal arm (*white,* decreased copy number; *black,* increased copy number; *gray,* no change). *B,* Kaplan-Meier survival plot showing association between aneuploidy and clinical outcome. Aneuploidy measured as percentage of nondiploid chromosomal arms (low aneuploidy group, $n = 8$; high aneuploidy group, $n = 41$).

[3] http://www.spotfire.com
[4] http://www-stat.stanford.edu/~tibs/SAM/
[5] http://www.broad.mit.edu/cancer/
[6] http://www.broad.mit.edu/gsea/msigdb/msigdb_index.html

Table 1. Kaplan-Meier survival analysis based on aneuploidy

Comparison based on percentage of nondiploid chromosomal arms	Association with survival (*P*)
≤5% (*n* = 8 tumors) vs. >5% (*n* = 41 tumors)	0.05
≤10% (*n* = 18 tumors) vs. >10% (*n* = 31 tumors)	0.57
≤20% (*n* = 37 tumors) vs. >20% (*n* = 12 tumors)	0.59
≤25% (*n* = 44 tumors) vs. >25% (*n* = 5 tumors)	0.54

frequently altered chromosomal arms: 1p (loss in 27% of tumors), 3p (loss in 45%), 3q (loss in 49%), 6p (gain in 39%), 6q (loss in 39%), 8p (gain in 20% and loss in 20%), and 8q (gain in 69%). A similar spectrum of chromosomal alterations was observed in 336 published cases: 1- (22%), 3- (49%), 6p+ (18%), 6q- (17.9%), and 8q+ (35%). The other cluster consisted of the remaining chromosomal arms, which were altered less frequently and in a more random fashion. To determine whether additional subclusters of chromosomal CNVs could be identified, a self-organizing map was performed using an expanded 4 × 4 grid (Fig. 2A). Chromosomal alterations clustered around two opposite poles represented by 6p/6q and 3p/3q/8q. Changes on chromosomes 8p and 1p clustered closely to the 3p/3q/8q pole. Based on these findings, the status of chromosomes 3 and 6p allowed tumors to be classified into three major subgroups, with 3- and 6p+ tumors being almost mutually exclusive (Fig. 2B). Gene expression profiles of five $3^{nl}/6p^{nl}$ tumors, eight $3^{nl}/6p+$ tumors, and twelve 3- tumors were obtained using the Illumina Ref8 BeadChip array and analyzed for clustering using principal component analysis (Fig. 2C). Using this unsupervised technique, the $3^{nl}/6p^{nl}$ and $3^{nl}/6p+$ tumors formed one cluster,

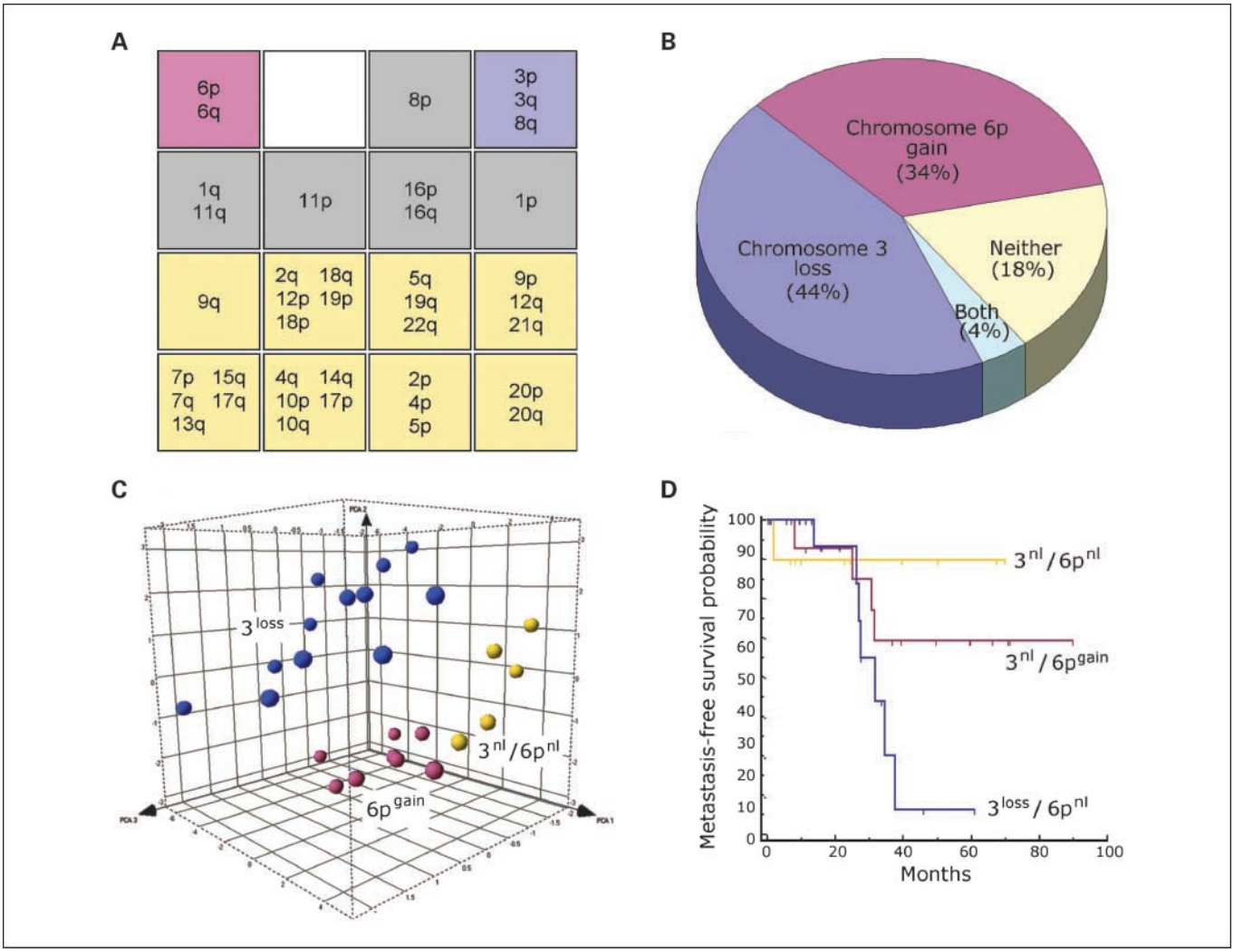

Fig. 2. Integrative genomic analysis reveals three major subgroups of tumors based on the status of chromosomes 3 and 6p. *A,* summary of SOM results using a 4 × 4 grid to cluster chromosomal arms on the basis of CNVs (absent or present). The proximity between boxes is proportional to the similarity in CNV patterns. Three main clusters were identified: 6p/6q (*lavender*), 3p/3q/8q (*blue*), and chromosomal arms with very low CNV (≤12% nondiploid chromosomal arms; *tan*). *B,* classification of tumors into three major subgroups based on the status of chromosomes 3 and 6p. *C,* principal component analysis based on gene expression profiling, showing the first three principal components in three-dimensional projection. Tan spheres, tumors with normal copy number for chromosomes 3 and 6p; lavender spheres, tumors with 6p gain; blue spheres, tumors with chromosome 3 loss. The proximity of spheres to each other is proportional to the similarity in their gene expression profiles. *D,* Kaplan-Meier survival chart showing the association of the three tumor subgroups with clinical outcome.

and the 3- tumors formed another cluster, consistent with our previous work (23). Interestingly, however, the $3^{nl}/6p^{nl}$ and $3^{nl}/6p+$ tumors further segregated into distinct subgroups. Thus, classifying tumors based on chromosome 3 and 6p status seemed to have a biologically relevant basis because the same groupings could be obtained based on gene expression profiles. Furthermore, the classification was prognostically significant, with $3^{nl}/6p^{nl}$, $3^{nl}/6p+$, and 3- tumors having progressively greater metastatic risks (Fig. 2D).

Of the seven frequently altered chromosomal arms, all were associated with overall aneuploidy except 6p+ (Fig. 3A). The strongest associations with aneuploidy were observed for 8p+, 8p-, and 8q+ ($P < 0.0001$ for each). Similar results were observed for the 336 published cases (Fig. 3B). Because 8p+,

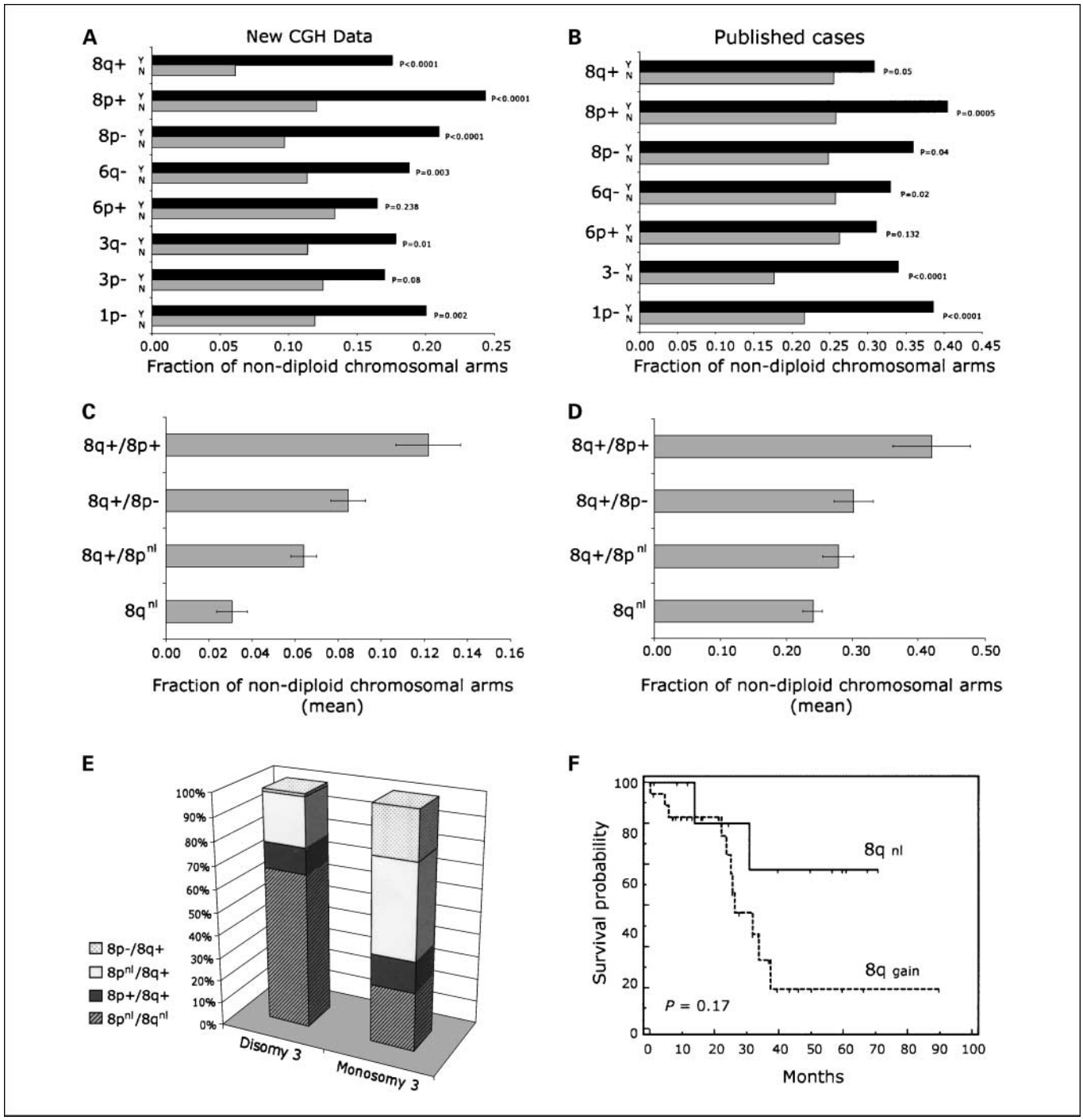

Fig. 3. Analysis of frequently altered chromosomal arms. *A,* association between frequently altered chromosomal arms and overall aneuploidy (fraction of nondiploid chromosomal arms) for the 49 primary UMs analyzed by array CGH (*columns*). *B,* association between frequently altered chromosomal arms and overall aneuploidy for the 336 published cases (*columns*). *C,* relationship between chromosome 8 status and overall aneuploidy in the 49 primary UMs analyzed by array CGH (*columns*). *D,* relationship between chromosome 8 status and overall aneuploidy in the 336 published cases (*columns*). *E,* spectrum of chromosome 8p and 8q changes with respect to chromosome 3 status in the 336 published cases. *F,* Kaplan-Meier survival plot showing association between 8q status and clinical outcome.

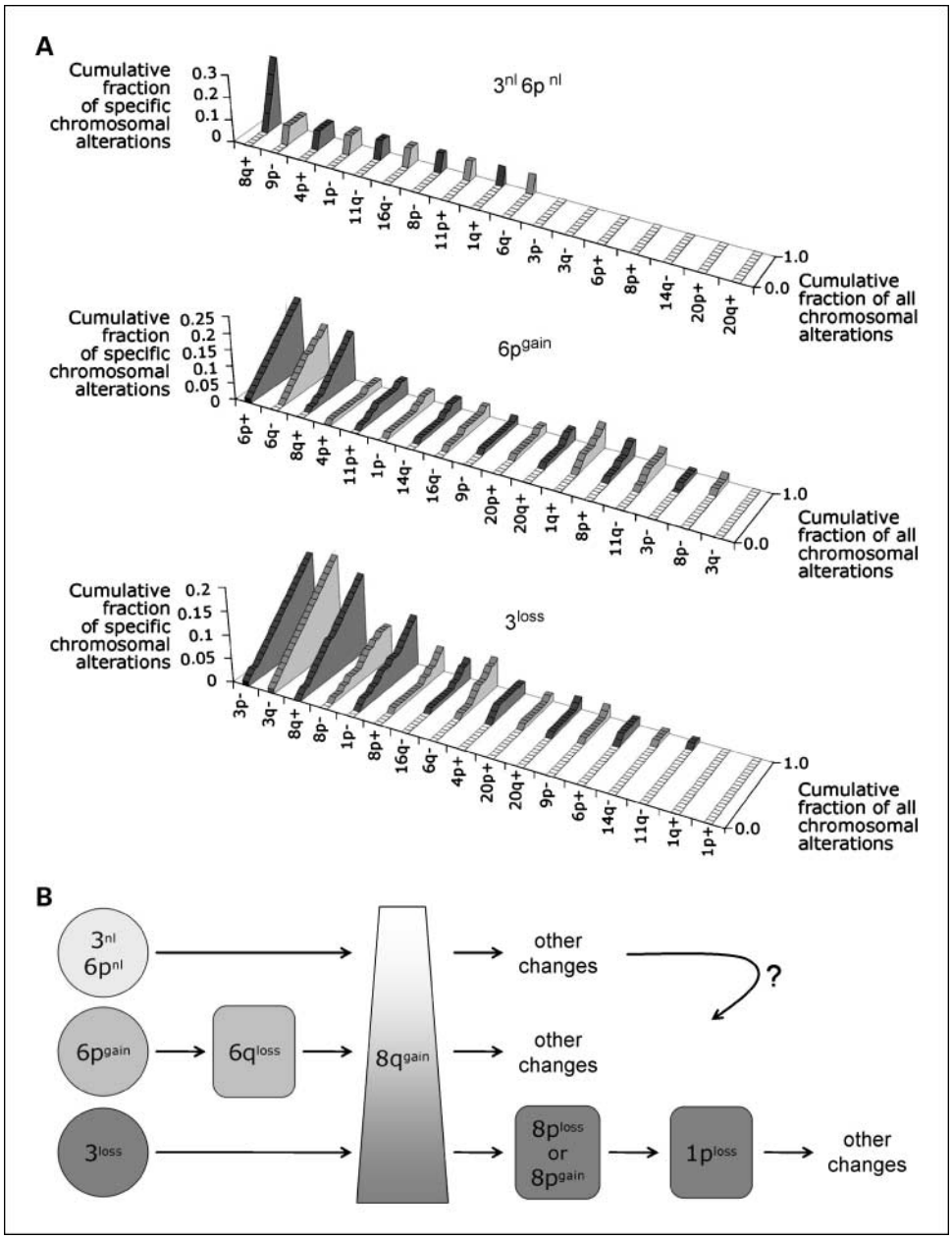

Fig. 4. Temporal sequence of chromosomal alterations. *A,* cumulative fraction of alterations in specific chromosomal arms as a function of overall aneuploidy in the three major tumor subgroups ($3^{nl}/6p^{nl}$, 6p+, and 3-). *B,* three hypothesized pathogenetic sequences of UM progression.

8q+, and 8p- involve the same chromosome and are thus not independent of each other, a subanalysis of these alterations was done. The combination of chromosome 8 alterations that was most strongly associated with aneuploidy was 8p+/8q+ (consistent with trisomy 8), followed by 8p-/8q+ (consistent with isochromosome 8q; Fig. 3C-D). Simple 8q gain showed the weakest association with aneuploidy. The spectrum of chromosome 8 alterations in disomy 3 tumors was significantly different than in monosomy 3 tumors (Fig. 3E). In particular, 8p-/8q+ (presumably due to isochromosome 8q) occurred almost exclusively in 3- tumors. Nonetheless, the status of 8q did not achieve statistical significance as a prognostic factor ($P = 0.17$; Fig. 3F).

Because aneuploidy is thought to accumulate in a unidirectional manner with respect to time, the number of CNVs can be used as a temporal measure of tumor progression to identify early versus late chromosomal alterations (2). Our 49 UMs were ordered on the basis of overall aneuploidy and then analyzed for enrichment for specific chromosomal alterations at the low versus high end of the aneuploidy scale. The cumulative fraction of specific chromosomal arm CNVs was plotted against the fraction of nondiploid chromosomal arms per tumor. For $3^{nl}/6p^{nl}$ tumors ($n = 10$), aneuploidy was very low (Fig. 4A). 8q+ was the most consistent alteration in this subgroup. For $3^{nl}/6p+$ tumors ($n = 17$), early alterations included 6q- followed by 8q+. For 3- tumors ($n = 22$), the earliest alteration was 8q+, followed by 8p- and 1p. These findings suggest the existence of at least two genetic sequences, with 3- and 6p+ representing alternative early events (Fig. 4B). $3^{nl}/6p^{nl}$ tumors could represent a third sequence or an early manifestation of one of the other two sequences. Even

though 8q+ was most strongly associated with 3- tumors, it also occurred commonly in the other two subgroups, suggesting that this gain of one or more loci on 8q may be important for tumor progression in all subgroups of UM. The ubiquity of 8q+ could also explain why it was not predictive of patient outcome (Kaplan-Meier, $P = 0.268$).

We previously described a molecular classification based on gene expression profiling that accurately predicts clinical outcome in UM (23), and class assignments were available for 43 of the tumors in this study. Aneuploidy was significantly associated with the poor prognosis class 2 signature; all tumors with the favorable class 1 signature exhibited low aneuploidy (<5% nondiploid chromosomal arms), whereas 57% of tumors with the class 2 signature exhibited higher levels of aneuploidy (>5% nondiploid chromosomal arms; Fisher exact test, $P = 0.004$).

To further explore gene expression patterns associated with aneuploidy, five tumors with low aneuploidy (<5% nondiploid chromosomal arms; MM49, MM18, MM57, MM74, and MM94) and four tumors with high aneuploidy (>20% nondiploid chromosomal arms; MM55, MM64, MM76, and MM92) and were analyzed using Illumina Human Ref8 BeadChip arrays, and 54 differentially expressed genes were identified using SAM (Fig. 5A). This list included genes involved in cell cycle regulation (*PTEN*, *PDGFD*, *CGRRF1*, *HDGFRP3*, and *NEK1*), centrosome function (*PTEN*, *CP110*, *TUBGCP3*, *SPG20*, and *NEK1*), and DNA damage repair (*ATR* and *NEK1*). Interestingly, only 22% of the genes in this list are located on the seven frequently altered chromosomal arms described earlier. The 54-gene set was analyzed with the Gene Set Analysis module of SAM to identify significant associations with curated gene sets (Supplementary Table S2). For genes that were up-regulated in high-aneuploidy tumors, there was a significant overlap with genes up-regulated in breast cancer, multiple myeloma, keratinocytes treated with UVB irradiation, and with cell cycle genes. For genes that were down-regulated in high-aneuploidy tumors, there was significant overlap with genes that were down-regulated in hepatocellular carcinomas induced with the genotoxic carcinogen diethylnitrosamine and genes that were epigenetically silenced in colon cancer. One of the discriminating genes was the tumor suppressor *PTEN*, which has a role in the maintenance of genome integrity (24). To validate the association between *PTEN* expression and aneuploidy, an independent set of 16 primary UMs and 3 normal uveal melanocyte cell lines were analyzed on the Affymetrix U133A platform, which confirmed that *PTEN* expression was strongly associated with increased aneuploidy (Pearson correlation, $P = 0.003$; Fig. 5B).

Discussion

In this study, aneuploidy patterns were studied in 388 primary UMs. The karyotypic changes in UM are generally less complex than in some other solid tumors, such as lung and breast cancer, possibly because UM is diagnosed at an earlier stage due to its sensitive location within the eye. The less complex karyotypic changes of UM allow earlier, and potentially more pathogenetically relevant, changes to be identified. The main findings of this study were that: (*a*) discrete chromosomal alterations tended to occur in specific clusters,

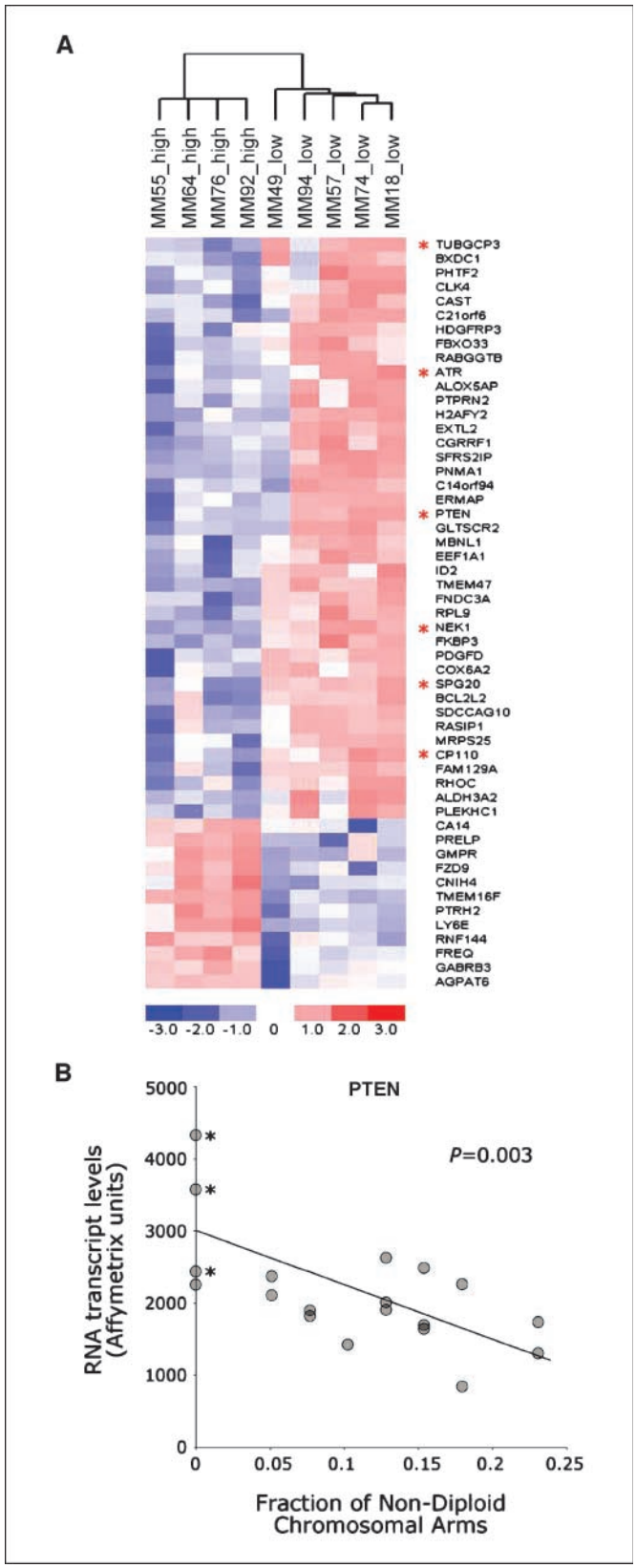

Fig. 5. Gene expression signature of aneuploidy. *A,* heatmap of tumors with high aneuploidy (*left*) and low aneuploidy (*right*) investigated with Illumina Ref8 BeadChip arrays and analyzed with Dchip software. Genes that have been reported to have a role in genomic integrity (*red asterisk*). *B,* validation of association between PTEN expression, measured on the Affymetrix U133 GeneChip array, and overall aneuploidy in normal uveal melanocytes (*asterisks*) and 16 primary UMs.

(*b*) these alterations tended to accumulate in a nonrandom temporal sequence, with the association between aneuploidy and poor clinical outcome driven by early chromosomal alterations rather than overall aneuploidy, (*c*) tumors could be classified into three prognostically significant groups based on the status of chromosomes 3 and 6p, and (*d*) aneuploidy was associated with a gene expression signature enriched for genes that regulate genomic integrity.

Although other studies have identified discrete patterns of chromosomal alterations in UM (4, 12, 14, 20, 22), this study used statistical "pattern recognition" techniques to organize chromosomal alterations into significant groupings. This analysis confirmed that 3- and 6p+ represent almost mutually exclusive alterations and thereby provided further support to the idea that 3- and 6p+ signify alternative pathogenetic sequences, as previously suggested (22, 25, 26). In addition, we identified a third subgroup, representing ~18% of all tumors, which were normal for chromosomes 3 and 6p. Gene expression profiling suggested that this subgroup was genetically more similar to the 6p+ tumors than to the 3- tumors and, thus, may represent an earlier stage in the 6p+ pathogenetic sequence. In any event, $3^{nl}/6p^{nl}$ tumors exhibited a better prognosis than the 6p+ tumors, indicating that it is clinically relevant to distinguish between these two subgroups.

Although 8q+ was most strongly associated with 3- tumors, this alteration was also found in 6p+ and $3^{nl}/6p^{nl}$ tumors. This may explain why 8q+ did not achieve statistical significance as a predictor of clinical outcome. The ubiquity of 8q+ also suggests that there may be a strong selective pressure for gain of genetic material on 8q in all UM pathogenetic sequences. Several oncogenes are located on 8q and are frequently up-regulated in UM, including *MYC*, *DDEF1*, and *NBS1* (27–29). The spectrum of chromosome 8 abnormalities was different between the main tumor subgroups. One particular abnormality, 8p-/8q+, which is consistent with isochromosome 8q (17, 30), was more common in 3- tumors and tended to occur later than simple 8q gain (Fig. 4A-B). Consistent with 8p loss being a later event in tumor progression, we recently identified a metastasis modifier locus on 8p that is deleted in tumors with more rapid onset of metastasis.[7]

We studied the temporal sequence in which chromosomal alterations accumulated in individual tumors, based on the assumption that aneuploidy accrues over time, with more advanced tumors having more aneuploidy than less advanced tumors (2). A similar analysis was done in UM (26), but this previous study relied on karyotype analysis of cultured tumor cells, which could be associated with cell culture artifacts and does not provide the same resolution as microarray-based genome-wide techniques. In this study, we used array comparative genomic hybridization to analyze primary tumor samples. 3- and 6p+ seemed to be early events in their respective sequences, with 8q+ being a later event (Fig. 4A-B). This was consistent with the previous suggestion that 8q+ occurs after 3- and 6p+ (25). In 6p+ tumors, 6q- and 8q+ were the most common subsequent events, with the coexistence of 6p+ and 6q- in the same tumor likely representing isochromosome 6p (15). In 3- tumors, 8q+ was the most common subsequent event, followed by 8p- or 8p+ then 1p-. The alterations on 1p and 8p were fairly specific to 3- tumors. Overall, 3- tumors exhibited more aneuploidy than the other two subgroups.

The gene expression signature of aneuploidy revealed a significant enrichment for genes involved in centrosome function, cell cycle regulation, and DNA damage repair, which are key functions associated with the maintenance of genomic integrity. Furthermore, there was a significant overlap between the genes in this signature and the curated gene sets associated with UVB irradiation (UVB_NHEK3_C3; ref. 31). and the genotoxic agent diethylnitrosamine (LEE_DENA_DN; ref. 32), further linking this signature to DNA damage and genomic integrity. These results parallel recent work that identified a gene expression signature associated with aneuploidy in six different cancer types, containing genes involved in chromosomal regulation and genomic integrity (33). Because this previous study did not analyze aneuploidy directly but used a surrogate measure based on gene expression profiling, our findings based on direct analysis of DNA copy number provides important confirmation of these previous findings in a different cancer type.

Down-regulated genes in our aneuploidy signature included *CP110*, which coordinates cell cycle progression with centrosome duplication (34), and *NEK1*, which is also involved with centrosomal function and in the response to DNA damage induced by ionizing radiation (35). Another down-regulated gene was *ATR*, the mutation of which leads to microsatellite instability (36). Furthermore, fragile sites are thought to be unreplicated chromosomal regions resulting from stalled replication forks that escape the ATR replication checkpoint (37). Because *ATR* is located at chromosome 3q22, it is interesting to speculate that this could explain, at least in part, the increased overall aneuploidy in 3- tumors. Perhaps the most interesting gene that was down-regulated in the aneuploidy signature was *PTEN*, which is a known tumor suppressor that was recently shown to be mutated and associated with poor clinical outcome in UM (38).

PTEN plays a fundamental role in the maintenance of chromosomal stability through the physical interaction with centromeres and control of DNA repair, and it has been implicated as an important guardian of genomic integrity (24). Loss of PTEN promotes genomic instability through several mechanisms. PTEN loss causes activation of AKT and impairment of CHK1 function (39). PTEN localizes to centromeres and physically associates with CENP-C, an integral component of the kinetochore, and it regulates the expression of Rad51, which reduces the incidence of spontaneous double-strand breaks. It is interesting to speculate that a reduction in Rad51, as a consequence of PTEN loss, might create selective pressure to amplify the parallel NBS1/Rad50 DNA damage repair pathway, which is often observed in UM (27).

The results of this study provide new insights into the relationship between aneuploidy and clinical outcome while confirming the existence of discrete tumor phenotypes containing distinct sets of chromosomal alterations. This study supports the nonrandom temporal nature of these cytogenetic changes and identifies several genes, including *PTEN*, which may play a fundamental role in aneuploidy and genomic stability.

[7] M.D. Onken and J.W. Harbour, unpublished data.

References

1. Lengauer C, Kinzler KW, Vogelstein B. Genetic instabilities in human cancers. Nature 1998;396:643–9.
2. Hoglund M, Gisselsson D, Sall T, Mitelman F. Coping with complexity. multivariate analysis of tumor karyotypes. Cancer Genet Cytogenet 2002;135:103–9.
3. Lee J, Kotliarova S, Kotliarov Y, et al. Tumor stem cells derived from glioblastomas cultured in bFGF and EGF more closely mirror the phenotype and genotype of primary tumors than do serum-cultured cell lines. Cancer Cell 2006;9:391–403.
4. Ehlers JP, Harbour JW. Molecular pathobiology of uveal melanoma. Int Ophthalmol Clin 2006;46:167–80.
5. Harbour JW. Clinical overview of uveal melanoma: introduction to tumors of the eye. In: Albert DM, Polans A, editors. Ocular Oncology. New York: Marcel Dekker; 2003. p. 1–18.
6. Cross NA, Murray AK, Rennie IG, Ganesh A, Sisley K. Instability of microsatellites is an infrequent event in uveal melanoma. Melanoma Res 2003;13:435–40.
7. Papadopoulos S, Benter T, Anastassiou G, et al. Assessment of genomic instability in breast cancer and uveal melanoma by random amplified polymorphic DNA analysis. Int J Cancer 2002;99:193–200.
8. Worley LA, Onken MD, Person E, et al. Transcriptomic versus chromosomal prognostic markers and clinical outcome in uveal melanoma. Clin Cancer Res 2007; 13:1466–71.
9. Onken MD, Worley LA, Person E, Char DH, Bowcock AM, Harbour JW. Loss of heterozygosity of chromosome 3 detected with single nucleotide polymorphisms is superior to monosomy 3 for predicting metastasis in uveal melanoma. Clin Cancer Res 2007; 13:2923–7.
10. Sisley K, Rennie IG, Parsons MA, et al. Abnormalities of chromosomes 3 and 8 in posterior uveal melanoma correlate with prognosis. Genes Chromosomes Cancer 1997;19:22–8.
11. White VA, Chambers JD, Courtright PD, Chang WY, Horsman DE. Correlation of cytogenetic abnormalities with the outcome of patients with uveal melanoma. Cancer 1998;83:354–9.
12. Sisley K, Parsons MA, Garnham J, et al. Association of specific chromosome alterations with tumour phenotype in posterior uveal melanoma. Br J Cancer 2000;82:330–8.
13. Speicher MR, Prescher G, du Manoir S, et al. Chromosomal gains and losses in uveal melanomas detected by comparative genomic hybridization. Cancer Res 1994;54:3817–23.
14. Kilic E, van Gils W, Lodder E, et al. Clinical and cytogenetic analyses in uveal melanoma. Invest Ophthalmol Vis Sci 2006;47:3703–7.
15. Aalto Y, Eriksson L, Seregard S, Larsson O, Knuutila S. Concomitant loss of chromosome 3 and whole arm losses and gains of chromosome 1, 6, or 8 in metastasizing primary uveal melanoma. Invest Ophthalmol Vis Sci 2001;42:313–7.
16. Wiltshire RN, Elner VM, Dennis T, Vine AK, Trent JM. Cytogenetic analysis of posterior uveal melanoma. Cancer Genet Cytogenet 1993;66:47–53.
17. Prescher G, Bornfeld N, Friedrichs W, Seeber S, Becher R. Cytogenetics of twelve cases of uveal melanoma and patterns of nonrandom anomalies and isochromosome formation. Cancer Genet Cytogenet 1995;80:40–6.
18. Naus NC, Verhoeven AC, van Drunen E, et al. Detection of genetic prognostic markers in uveal melanoma biopsies using fluorescence *in situ* hybridization. Clin Cancer Res 2002;8:534–9.
19. van den Aardweg GJ, Kilic E, de Klein A, Luyten GP. Dose fractionation effects in primary and metastatic human uveal melanoma cell lines. Invest Ophthalmol Vis Sci 2003;44:4660–4.
20. Tschentscher F, Prescher G, Zeschnigk M, Horsthemke B, Lohmann DR. Identification of chromosomes 3, 6, and 8 aberrations in uveal melanoma by microsatellite analysis in comparison to comparative genomic hybridization. Cancer Genet Cytogenet 2000; 122:13–7.
21. Scholes AG, Liloglou T, Maloney P, et al. Loss of heterozygosity on chromosomes 3, 9, 13, and 17, including the retinoblastoma locus, in uveal melanoma. Invest Ophthalmol Vis Sci 2001;42:2472–7.
22. Hughes S, Damato BE, Giddings I, Hiscott PS, Humphreys J, Houlston RS. Microarray comparative genomic hybridisation analysis of intraocular uveal melanomas identifies distinctive imbalances associated with loss of chromosome 3. Br J Cancer 2005;93: 1191–6.
23. Onken MD, Worley LA, Ehlers JP, Harbour JW. Gene expression profiling in uveal melanoma reveals two molecular classes and predicts metastatic death. Cancer Res 2004;64:7205–9.
24. Shen WH, Balajee AS, Wang J, et al. Essential role for nuclear PTEN in maintaining chromosomal integrity. Cell 2007;128:157–70.
25. Parrella P, Sidransky D, Merbs SL. Allelotype of posterior uveal melanoma: implications for a bifurcated tumor progression pathway. Cancer Res 1999;59: 3032–7.
26. Hoglund M, Gisselsson D, Hansen GB, et al. Dissecting karyotypic patterns in malignant melanomas: temporal clustering of losses and gains in melanoma karyotypic evolution. Int J Cancer 2004;108:57–65.
27. Ehlers JP, Harbour JW. NBS1 expression as a prognostic marker in uveal melanoma. Clin Cancer Res 2005;11:1849–53.
28. Ehlers JP, Worley L, Onken MD, Harbour JW. DDEF1 is located in an amplified region of chromosome 8q and is overexpressed in uveal melanoma. Clin Cancer Res 2005;11:3609–13.
29. Parrella P, Caballero OL, Sidransky D, Merbs SL. Detection of c-myc amplification in uveal melanoma by fluorescent in situ hybridization. Invest Ophthalmol Vis Sci 2001;42:1679–84.
30. Horsman DE, Sroka H, Rootman J, White VA. Monosomy 3 and isochromosome 8q in a uveal melanoma. Cancer Genet Cytogenet 1990;45: 249–53.
31. Sesto A, Navarro M, Burslem F, Jorcano JL. Analysis of the ultraviolet B response in primary human keratinocytes using oligonucleotide microarrays. Proc Natl Acad Sci U S A 2002;99:2965–70.
32. Lee JS, Chu IS, Mikaelyan A, et al. Application of comparative functional genomics to identify best-fit mouse models to study human cancer. Nat Genet 2004;36:1306–11.
33. Carter SL, Eklund AC, Kohane IS, Harris LN, Szallasi Z. A signature of chromosomal instability inferred from gene expression profiles predicts clinical outcome in multiple human cancers. Nat Genet 2006;38:1043–8.
34. Chen Z, Indjeian VB, McManus M, Wang L, Dynlacht BD. CP110, a cell cycle-dependent CDK substrate, regulates centrosome duplication in human cells. Dev Cell 2002;3:339–50.
35. Polci R, Peng A, Chen PL, Riley DJ, Chen Y. NIMA-related protein kinase 1 is involved early in the ionizing radiation-induced DNA damage response. Cancer Res 2004;64:8800–3.
36. Menoyo A, Alazzouzi H, Espin E, Armengol M, Yamamoto H, Schwartz S, Jr. Somatic mutations in the DNA damage-response genes ATR and CHK1 in sporadic stomach tumors with microsatellite instability. Cancer Res 2001;61:7727–30.
37. Casper AM, Nghiem P, Arlt MF, Glover TW. ATR regulates fragile site stability. Cell 2002;111: 779–89.
38. Abdel-Rahman MH, Yang Y, Zhou XP, Craig EL, Davidorf FH, Eng C. High frequency of submicroscopic hemizygous deletion is a major mechanism of loss of expression of PTEN in uveal melanoma. J Clin Oncol 2006;24:288–95.
39. Puc J, Keniry M, Li HS, et al. Lack of PTEN sequesters CHK1 and initiates genetic instability. Cancer Cell 2005;7:193–204.